Research Article

Reprogramming MAO-A-Driven Oxidative Stress: Computational Discovery of Neuroprotective Leads for Diabetic Neuropathy

Gowdham Manivel[1] | Shanmughavel Piramanayagam[1] |

1. Department of Bioinformatics, Bharathiar University, Coimbatore, Tamil Nadu, India

Abstract

Diabetic Neuropathy (DN) is a severe diabetes complication linked to progressive peripheral nerve degeneration, oxidative stress, mitochondrial dysfunction and chronic neuropathic pain with no effective disease-modifying therapies available to date. Due to the key role of MAO-A in monoamine metabolism and reactive oxygen species production, its inhibition may help reduce oxidative stress–related neuronal damage in diabetic neuropathy. This study used a computational drug discovery approach targeting MAO-A. Ligand-based pharmacophore modeling was performed using 52 caffeine derivatives from the literature to create a dataset for energetic evaluation and identify new MAO-A inhibitors. A five-feature AAHRR hypothesis comprising two hydrogen bond acceptors, one hydrophobic and two aromatic rings was generated using the PHASE 3.0 module. A series of these 1,000 drug-like compounds were then retrieved by screening the ZINC database with validated pharmacophore model. They underwent molecular docking and high-throughput virtual screening against the human MAO-A crystal structure (PDB ID: 2Z5X). Among 591 compounds with appropriate binding profiles, the top ranked compound based on Glide G score was ZINC02123682 [(1r,4r)-4-((2-(5,7-dimethoxy-4-methyl-2-oxo-2H-chromen–3–yl) acetamido) methyl) cyclohexane carboxylic acid] (Glide G-score = −7.54). The stability of the protein–ligand complex was additionally validated by 1000-ps molecular dynamics simulations in explicit TIP3P water environment using the OPLS_2005 force field, with stable RMSD fluctuations maintained within 2-4 Å and a favourable negative potential energy profile through the period of simulation. These data characterize ZINC02123682 as a structurally optimized and dynamically stable MAO-A inhibitor, providing an attractive lead compound in the development of potential new neuroprotective therapeutics for diabetic neuropathy.

1. Introduction

Diabetic neuropathy (DN) is one of the most common and severe chronic complications of diabetes mellitus, which nearly half of the diabetic patients will suffer in the whole life cycle **(Gupta *et al.* 2026)**. The progressive loss of sensory function, neuropathic pain, motor dysfunction and autonomic impairment in DN severely impacts on quality of life and remains a major global healthcare problem **(Yang *et al.* 2025)**. DN is characterized by a complex pathogenesis and multifactorial nature; persistent hyperglycemia, oxidative stress, mitochondrial dysfunction, neuroinflammation and microvascular insufficiency are involved in the intricate pathophysiological cascade of the disease **(Samsu 2021)**. Chronic metabolic abnormalities induce overproduction of reactive oxygen species (ROS), and impair neuronal energy metabolism and neurovascular homeostasis ultimately resulting in axonal degeneration and neuronal apoptosis **(Picca *et al.* 2020)**. Although effective methods for glycemic control have been developed and substantial progress has been made in the management of diabetes, treatment options to slow or halt DN are still relatively limited, primarily involving symptomatic intervention with analgesics (includes anticonvulsants and antidepressant therapies) or combination regimens mostly based on opioid drugs which provide only moderate efficacy but do not correct the underlying neurodegenerative changes **(Tavafi 2013)**. As a result, the identification of new molecular targets in terms of modulating disease progression in diabetes continues to be a major focus for diabetic neuropathy research. Monoamine Oxidases (MAOs), a family of structurally and functionally related enzymes, have recently emerged as important targets in neurodegenerative and neuropathic disorders because they play central roles in neurotransmitter metabolism and maintaining oxidative homeostasis **(Yeung *et al.* 2019)**. MAOs are mitochondrial enzymes that dependent on flavin adenine dinucleotide and mediate oxidative deamination of a specific subset of biogenic amines such as serotonin, dopamine and norepinephrine **(Graves *et al.* 2020)**. MAO is composed of two isoforms, MAO-A and MAO-B, which have different substrate specificities and tissue distributions; specifically, MAO-A has higher expression levels in neuronal tissues and preferentially metabolizes serotonin (5-HT) and norepinephrine **(Kaludercic *et al.* 2014b)**.

On note, MAO-initiated catabolism produces the by-products hydrogen peroxide and reactive aldehyde intermediates which directly lead to oxidative stress and mitochondrial damage **(Kaludercic *et al.* 2014a)**. Excessive MAO-A activity also drives neuronal vulnerability through increased generation of reactive oxygen species, neurotransmitter imbalance, mitochondrial dysfunction and pro-inflammatory signalling pathways **(Maggiorani *et al.* 2017)**. Several of these mechanisms converge with fundamental pathological processes behind diabetic neuropathy, supporting the opportunity to study MAO-A inhibition as a neuroprotective approach. Selective inhibition of MAO-A represents an attractive therapeutic strategy to reduce oxidative stress while maintaining normal neuronal functions and neurotransmitter equilibrium. Mounting evidence supports that dysregulation of monoamine oxidase activity contributes to pathogenic processes in the development of diabetic complications, particularly via elevated production of reactive oxygen species (ROS) and mitochondrial injury **(Song *et al.* 2026)**. MAO-A mediates oxidative deamination of monoamine neurotransmitters that generates hydrogen peroxide and reactive aldehyde intermediates as byproducts, which can subsequently increase the oxidative stress, inflammatory signalling and cellular damage. Elevated oxidative load has been directly linked to mitochondrial dysfunction, propagation of abnormalities in axonal maintenance and neurodegenerative change, all relevant pathological characteristics of diabetic neuropathy in either nervous or non-nervous tissues **(Kaludercic *et al.* 2023)**.

Received on	:	2026-04-05	**Key Words:**
Revised on	:	2026-05-30	Diabetic Neuropathy
Accepted on	:	2026-06-16	Monoamine Oxidase A
Published Online	:	2026-07-28	Pharmacophore Modeling
Review Model	:	Single-Blind Review	Molecular Docking
No. of Reviewers	:	Two	MD Simulation
Edited by	:	Dr Chandrabose Selvaraj	Healthcare
Vol and Issue	:	02 (03)	Medicine
Page No	:	40-48	
Similarity Level	:	18% and 33% (AI)	DOI: 10.64659/jomi/225614
Correspondence	:	Dr. G. Manivel	**This article is licensed**
Contact Author	:	✉	

ISSN: 3108-2696 (Online)

The augmentation of oxidative stress markers and the enhancement of neuronal injury in diabetic experimental models exposed to chronic hyperglycemic conditions led to the hypothesis that ROS-generating enzymes may play a role in disease progression **(Gonzalez *et al.* 2023)**. Interestingly, MAO-A has also been involved in neurodegenerative and inflammatory conditions by modulating oxidative balance and mitochondrial homeostasis, which strengthens support for the therapeutic role of both enzymes in all pathological conditions involving neuronal dysfunction **(Kasznicki *et al.* 2012)**. Additionally, the clinical observation of increased oxidative stress associated with altered monoaminergic signaling and neuronal degeneration in diabetic complications makes MAO-A modulation a candidate approach for reducing oxidative damage to neurons. The role of MAO-A in the progression of diabetic neuropathy needs more experimental confirmation; hence we investigated computational agents as potential MAO-A targeted candidates to treatment **(Cagnin *et al.* 2022)**.

Although MAO-A inhibition is therapeutically desirable, consistent and effective selective activity against this enzyme is still being sought. While multiple MAO inhibitors have been developed for neurological diseases, selectivity for the different isoforms of MAO as well as potential side effects and long-term adverse effects are hindering a wider clinical use. Moreover, the structural and chemical diversity of putative MAO-A inhibitors has not yet been fully explored-calling for efficient computational techniques capable of recognizing new scaffolds with enhanced binding modalities and pharmacological profiles **(Hong and Li 2019)**. Ligand-based pharmacophore modeling, virtual screening, molecular docking and molecular dynamics simulations have evolved into powerful tools for accelerating lead discovery by allowing the systematic examination of large chemical libraries against biologically relevant targets **(Pal *et al.* 2019)**. In this regard, the current study was conducted to discover new MAO-A inhibitors for possible therapeutic application to diabetic neuropathy by an integrated computer-aided drug discovery approach. Ligand-based pharmacophore modeling of caffeine derivatives with different structures was performed to identify the important molecular features associated with inhibition of MAO-A. A chemically similar ZINC database was then screened using the resulting pharmacophore hypothesis **(Ranade *et al.* 2024)**. The obtained hits were assessed by means of molecular docking to the human MAO-A crystal structure, complemented by molecular dynamics simulations in order to investigate the stability and dynamic behavior of protein–ligand complexes under physiological conditions. The aim of this integrated computational workflow was to assist screening for novel lead compounds and help gain an understanding on their molecular properties that could potentially be used as neuroprotective agents in the treatment of diabetic neuropathy.

2. Materials and Methods

2.1. Target Acquisition and Protein Preparation

The crystallographic structure of human Monoamine Oxidase A (MAO-A) obtained from the RCSB Protein Data Bank **(PBD ID: 2Z5X)** was selected as the receptor model for the proposed molecular docking studies. The chosen structure was processed using the Protein Preparation Wizard module in Schrödinger Suite **(Son *et al.* 2008)**. The protein structure was first checked for missing atoms, incomplete side chains, alternate conformations and non-standard structural motifs. To decrease the complexity of our docking calculations, we have removed any crystallographic water molecules that were not involved in ligand recognition or stabilization **(Mukherjee *et al.* 2010)**. These calculations were performed in gas phase and hydrogen-atoms were added based on physiological protonation states (e.g., assignment of charged vs. neutral state of ionizable residues by Epik module at ~ physiologic pH). Orientations of hydroxyl groups, asparagine, glutamine and histidine residues were optimized to achieve an energetically favorable configurations at hydrogen-bonding networks. For side-chain atoms and residues that were deemed significant for structural integrity, missing values were repaired and optimized using the Prime module. According to chemical valence rules, bond orders, formal charges and atom types were corrected **(Johnston *et al.* 2023)**. The receptor structure was then minimized using the OPLS_2005 force field to relieve steric clashes and achieve a surfacel-less receptor geometry. The minimization was then performed to convergence, using the standard Schrödinger minimization protocol, with heavy atoms initially restrained to the experimental crystal conformation allowing for optimization of hydrogen positioning and local geometry. The minimized protein structure was then used for receptor grid generation and the molecular docking studies **(Ciancetta *et al.* 2017)**.

2.2. Ligand Dataset Construction & Activity Normalization

The list of 52 caffeine derivatives with experimentally determined MAO-A inhibitory activities was gathered from the literature. These IC_{50} values were subsequently converted into logs using the equation $pIC_{50} = -\log(IC_{50})$ to normalize activity values within disparate concentration ranges and enable pharmacophore generation. Compounds were classified into categories according to their inhibitory potency based on the activity classification criteria most used in ligand-based drug discovery studies **(Li *et al.* 2019)**. Compounds were designated as active (IC_{50} 5.0, inactive (IC_{50} >100 μM) when pIC_{50} values were <4.0 and moderately active if between those two limits. The method supports the retention of intermediate molecules in pharmacophore model generation while separating potent inhibitors from weakly active compounds. Activity binning strategies based on pIC_{50} thresholds have also been widely used in ligand-based pharmacophore modeling and virtual screening workflows. The curated dataset was then imported into the PHASE 3.0 module of Schrödinger Suite to generate the pharmacophore hypothesis **(Giordano *et al.* 2022)**.

2.3. Ligand Preparation and Conformational Analysis

Prior to the generation of pharmacophores, all ligands were prepared using the LigPrep module (Schrödinger). OPLS_2005 force field was used to perform geometry optimization. Hydrogens were added, ionization states assigned based on biologically relevant pH conditions, stereoisomers generated as appropriate and chemical inconsistencies corrected **(Alnajeebi 2026)**. Monte Carlo Multiple Minimum (MCMM) algorithm in the MacroModel module was employed for conformational sampling to accommodate ligand flexibility. This process produced a full conformer ensemble of energetically feasible ligand poses that can be used in the generation of pharmacophore hypotheses **(Olanders *et al.* 2020)**.

2.4. Pharmacophore Model Generation

The PHASE 3.0 from Schrödinger package was used for pharmacophore modeling. In the present study, six predefined pharmacophoric features were employed in model construction as: hydrogen bond acceptor (A), hydrogen bond donor (D), hydrophobic group (H), negatively charged group (N), positively charged group (P) and aromatic ring (R) **(Teli and K 2012)**. We identified common pharmacophores using tree-based partitioning of the set of active conformers. Evaluated hypotheses based on their quality of alignment, overlapping features, vector matching selectivity and conformational energies contributions. Scoring was enhanced with the inclusion of relative conformational energies and biological activity values to obtain better discrimination from SPM. The top-performing pharmacophore hypothesis is chosen for virtual screening experiments **(Ramachandran and Piramanyagam 2017)**.

2.5. Pharmacophore-Based Virtual Screening

The validated model was used as a three-dimensional query to carry out the virtual screening of ZINC chemical database using ZincPharmer

platform (**Poonia *et al.* 2023**). There were selections of screening parameters in a way that emphasizes on search for compounds with improved drug-like properties. Candidate molecules were filtered based on a maximum pharmacophore-matching root mean square deviation (RMSD) of 0.7 Å, ten or fewer rotatable bonds, molecular weight no more than 500 Da, hydrogen bond acceptors (HBA(s)) not larger than ten, hydrogen bond donors (HBD(s)) less than five, and calculated partition coefficient (logP) lower than five (**Rahimi and Abbasi 2026**). All the compounds fulfilling pharmacophoric and physicochemical constraints were kept for dockings (**Almars and Kattan 2025; Heider *et al.* 2023**).

2.6. Receptor Preparation and Grid Generation

The receptor grid (PDB ID: 2Z5X) was prepared from the MAO-A crystal structure using Glide Receptor Grid Generation module of the Schrödinger Suite. Active-site region was defined using the coordinates of co-crystallized ligands in the receptor structure (**Mateev *et al.* 2023**). After removing the ligand from the protein structure, a grid box centered on the native binding cavity of the receptor was constructed to generate bias for sampling of ligand poses in docking calculations (**Elokely and Doerksen 2013**). This kept the overall structural features of the receptor binding pocket intact, using default van der Waals scaling parameters. The generated receptor grid was then used for high throughput virtual screening and molecular docking studies (**Arcon *et al.* 2021**).

2.7. High-Throughput Virtual Screening

The selected compounds from the pharmacophore-based screening workflow, were further screened for structure-based virtual screening using Glide docking module of Schrödinger Suite. The Glide High-Throughput Virtual Screening (HTVS) mode was chosen because it allows many compounds to be processed rapidly (in the range of ~100,000–10,000 poses per hour), while providing an accurate and reliable prediction of ligand-receptor compatibility. This methodology was deemed suitable for chemical library screening to prioritize the pharmacophore matched candidates based on an in-depth follow-up analysis (**Mafethe *et al.* 2023**). Ligand conformation in the MAO-A binding site was modelled using flexible ligand docking. Spatial positions and orientations of the ligands were sampled when the docking poses were calculated, where receptor complementarity was evaluating upon Glide scoring function in our study. Compounds were ranked by their Glide G-score, a measure that estimates the relative binding favourability of each state based on hydrogen bonds with favourable geometry and intensity, hydrophobic interactions in solvent cavities, electrostatic contributions at the interface between two tips or between tip and surface, and ligand strain (**Coleman *et al.* 2013**). The top compounds were chosen based on good docking scores and interaction profiles for further analysis. For ZINC02123682 the reported Glide G-score at the time of this study (−7.54) relates to a previously performed docking using the Glide HTVS protocol. While higher precision modes including Glide SP and XP will likely produce even more well refined binding pose predictions, our choice of the HTVS approach was based on prioritization of pharmacophore-derived candidates from a very large virtual library that required fast calculation (**Huang *et al.* 2026**).

2.8. Molecular Dynamics Simulation

The most stable protein–ligand complex was analysed with the MacroModel module of the Schrödinger software suite. An explicit TIP3P water environment was used to solvate the receptor–ligand system to mimic physiological solvation (**Manish *et al.* 2022**). The system was then energy minimized using the Polak–Ribiere Conjugate Gradient (PRCG) algorithm with a maximum of 500 iterations converging at a threshold of 0.05 before each simulation. Simulations were conducted all using the OPLS_2005 force field (**Vilar *et al.* 2014**). Extended cutoff parameters were used to calculate long-range electrostatic and van der Waals interactions. In None, atomic coordinates, bond lengths, bond angles and dihedral angle position restraints were not imposed, and the None SHAKE option was used to allow free molecular motion (**Adcock and McCammon 2006**). The equilibration time was 1 ps, and then the molecular dynamics simulations at 300 K were obtained to assess their structural stability and dynamic behavior via monitoring of root mean square deviation (RMSD) profiles and potential energy fluctuations throughout the simulation trajectory (**Cediel-Becerra *et al.* 2025**).

3. Results

3.1. Structural Characterization of MAO-A

Monoamine Oxidase A (MAO-A) is a Mitochondrial, Flavin Adenine Dinucleotide-dependent enzyme involved in the oxidative deamination of several biogenic amines, having serotonin, norepinephrine and dopamine as substrate. In this way, MAO-A can cause oxidative stress and mitochondrial dysfunction by producing hydrogen peroxide and reactive aldehydes as metabolic substrates during a catalytic process. Objective Excessive monoamine oxidase A (MAO-A) activity contributes to the pathogenesis of diabetic neuropathy through neuronal oxidative damage, neuro inflammation, and abnormality of monoaminergic neurotransmission. Increased reactive oxygen species production due to chronic hyperglycemia causes functional impairment of neurons, leading to axonal degeneration and long-term peripheral nerve dysfunction. It is an attractive therapeutic target for disease-modifying interventions in diabetic neuropathy, given its dual role as a regulator of oxidative stress and neurotransmitter homeostasis. By decreasing oxidative burden and still maintaining neuronal signaling pathways, inhibiting MAO-A may indeed protect neurons from injury while also delaying the progression of these diseases. Therefore, the discovery of new MAO-A active site inhibitors may serve as a complementary approach to existing symptomatic pain treatments, which do not target the molecular-level mechanisms responsible for disease.

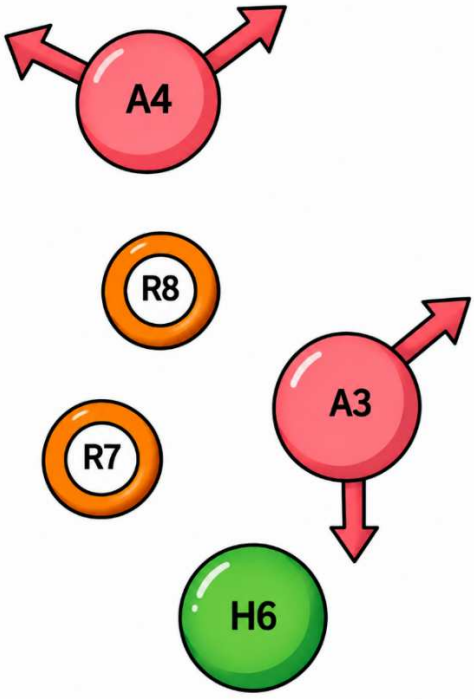

Figure 1. AAHRR common pharmacophore hypothesis.

3.2. Pharmacophore Fingerprinting and Hit Expansion

A pharmacophore modelling was first utilized on a dataset of 52 caffeine derivatives compiled from literature to identify more extensive, structural features necessary for the binding orienttation/interaction with MAO-A.

Ligand conformational space was exhaustively covered by expanding each compound into 1,825 energetically accessible conformers following LigPrep optimization and conformational sampling. Then, PHASE analysis yielded 272 pharmacophore hypotheses that were prioritized using survival scores based on geometric alignment along with feature overlap, vector match selectivity (VMS), biological activity information and conformational energy contributions **(Table S1 and Table 1)**. Out of the various models generated, the five-feature AAHRR pharmacophore hypothesis was revealed as both the most statistically robust and chemically relevant model **(Figure 1)**. The most promising hypothesis was a combination of two hydrogen-bond acceptor (HBA) features, one hydrophobic feature followed by two centers for an aromatic ring. The presence of hydrogen-bond acceptor functionalities points to the necessity of electron-rich areas for favourable interactions with respect to the MAO-A binding cavity. These polar interactions might stabilize the ligand using electrostatic contacts with the residues near to enzyme catalytic region. The hydrophobic property describes the extent of nonpolar contributions to saturation in lipophilic areas of the binding pocket and enhanced receptor complementarity. In turn, two aromatic ring features coincide with the spatially aromatic environments in MAO binding sites that we know are relatively rich in π–π stacking and van der Waals contributions to ligand stabilization.

Table 1: Alignment analysis of the selected AAHHR.59 pharmacophore hypothesis with representative ligands.

Ligand Name	Activity	Pharm Set	Fitness	Sites Matched	Relative Energy
3b.mol	6.150	active	2.72	5	4.946
3p5e	5.885	active	3.00	5	0.000
3p5d	5.874	active	3.00	5	0.000
3p5n	5.783	active	2.76	5	0.080
3p5M	5.738	active	2.75	5	0.079

To select hypotheses based on the AAHRR hypothesis, we first measured its predictive relevance by using PHASE-based internal scoring parameters that balance feature alignment and overlap quality with selectivity and energetic contributions. Out of alternatives generated hypotheses, the selected model showed better pharmacophoric arrangement suggesting its potential to be followed as a three-dimensional query for subsequent virtual screening. It must be mentioned that besides the performance of pharmacophore discrimination is measured in a quantitative manner by several additional retrospective validation methods such as receiver-operator characteristic (ROC) analysis, ROC-AUC, enrichment factor (EF), Güner–Henry (GH) score, BEDROC analysis and external decoy dataset validation. This type of analyses needs a correctly desecrated independent dataset that contains experimentally validated MAO-A inhibitors with varying levels of activity. Thus, the present AAHRR model that achieves internal consistency & has been validated in virtual screening needs external validation for further enhancement of its predictive reliability. Moreover, virtual screening was performed using the ZINC database under stringent pharmacophore matching and drug-likeness constraints that supported the biological relevance of the AAHRR model. Based on the pharmacophore RMSD criteria (≤2.5 Å), molecular weight (≤500 Da), restricted conformational flexibility and beneficial physicochemical properties, around 1,000 compounds were screened for obtaining the hits compatible with pharmacophore **(Table S2)**. Molecular diversity is one of the main features underlying the observed expansion in chemical space from the original training dataset of caffeine derived molecules to a wider virtual library and thus suggests that essential molecular interaction properties required for MAO-A binding were successfully captured by an AAHRR hypothesis. Compared to common MAO inhibitors, which typically act through covalent mechanisms or limited aromatic scaffolds, the AAHRR pharmacophore enables a large molecular scaffold for reversible inhibitor candidates that provide selectivity and better pharmacokinetics.

3.3. Molecular Docking Mechanics and Lead Selection

The pharmacophore-derived compounds were subjected to high-throughput virtual screening using the Glide HTVS docking protocol to evaluate their compatibility with the MAO-A binding site. Flexible ligand docking was performed to assess receptor–ligand complementarity, binding pose suitability, and energetic favorability. Progressive evaluation of the 591 pharmacophore-selected candidates using the Glide HTVS docking protocol and assessment of receptor complementarity, binding pose quality, and energetic favorability resulted in 591 compounds exhibiting acceptable docking characteristics. These compounds were further considered for ranking and identification of the highest-performing ligand **(Table S3)**. Among the screened compounds, ZINC02123682 emerged as the top-ranked candidate with a Glide G-score of −7.54. The compound demonstrated favorable alignment with the essential features of the AAHRR pharmacophore, including hydrogen-bond acceptor interactions, aromatic contributions, and hydrophobic complementarity within the MAO-A binding cavity. The docking pose indicated that ZINC02123682 was appropriately accommodated within the active-site region, supporting the pharmacophore-based prediction of favorable receptor recognition. The interaction profile of MAO-A with ZINC02123682 revealed stabilizing contacts with key binding-site residues, including ALA68, TYR69, and ARG51. The ligand established oxygen-mediated hydrogen-bond interactions with these residues, with interaction distances ranging from 1.98 Å to 2.26 Å **(Table 2, Figure 2)**. These interactions contribute to ligand stabilization and suggest effective occupation of the MAO-A catalytic region. The presence of complementary hydrogen-bonding and hydrophobic interactions supports the potential of ZINC02123682 to interfere with MAO-A substrate recognition and catalytic function. Mechanistically, inhibition of MAO-A may reduce oxidative stress-associated pathways by limiting the production of reactive oxygen species generated during monoamine metabolism. Therefore, the favorable docking score, pharmacophore compatibility, and binding interactions suggest that ZINC02123682 represents a potential lead scaffold for further investigation as a MAO-A inhibitor. However, biochemical enzyme inhibition assays, selectivity evaluation against MAO-B, and pharmacological validation are required to confirm its inhibitory activity and therapeutic relevance.

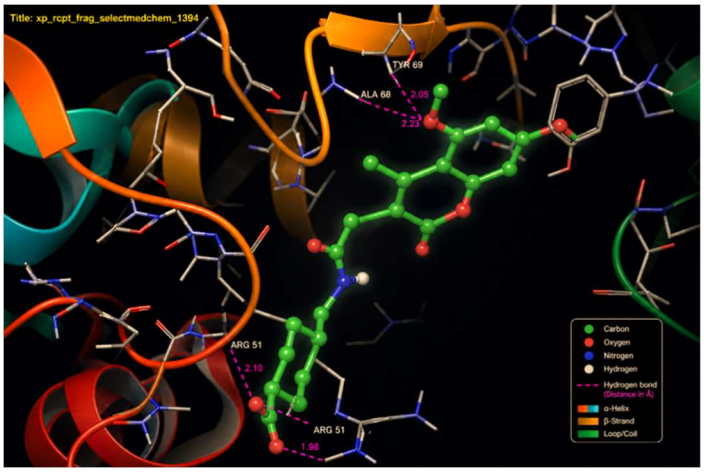

Figure 2. Ligand (ZINC02123682) and Protein (2Z5X) interaction.

3.4. Molecular Dynamics and Thermodynamic Stability

As docking presents a static aspect of receptor–ligand interactions, evaluation for stability of the protein–ligand ensemble due to dynamic wet solvent conditions is also essential to understand binding behaviour. For

evaluating the conformational stability of the best-scoring MAO-A–ZINC02123682 complex, molecular dynamics (MD) simulation was performed using Macro Model module of Schrödinger software suite in an explicit TIP3P water environment employing OPLS_2005 force field. The simulation runs for 1000 ps (1 ns) was designed to offer an order of magnitude estimate of the conformational stability and energetic profile of the protein–ligand complex at physiological conditions. The earlier aforementioned "very close to two microseconds" this simulation duration is since 1000 ps = 1 ns, however, two microseconds are equal with each other = 2000 ns, so that form record or refer wrongly. The structural stability of the protein–ligand complex was analyzed by tracking its RMSD over the simulation time, which indicated that the system settled in a stable conformation, maintaining overall root mean square deviations (RMSD) values within sinuously ~2 to 4 Å during most of the simulation timeframe. The little structure deviation indicates that the ligand remained bound in a similar orientation within the MAO-A active pocket during the MD simulation trajectory.

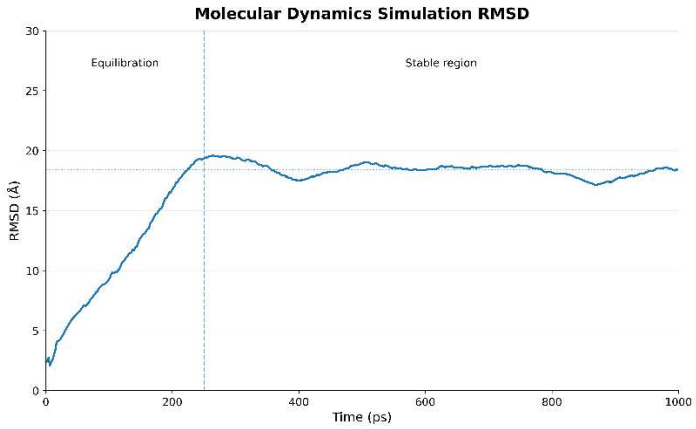

Figure 3a. RMSD analysis of the Protein-Ligand complex

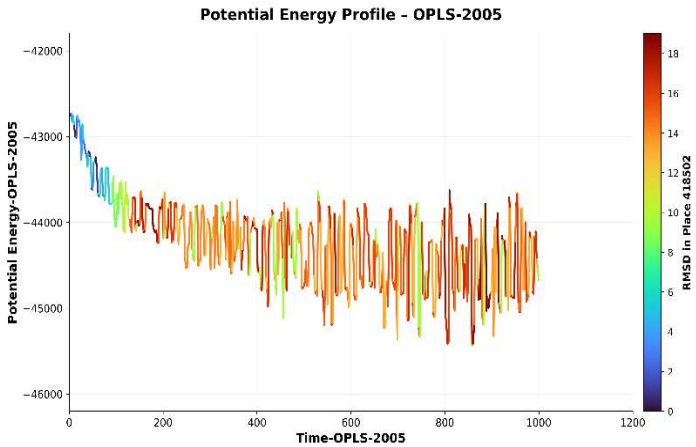

Figure 3b. Potential energy of the Protein-Ligand complex

Table 2: Ligand (ZINC02123682) and Protein (2Z5X) interaction

Amino Acid	Residue atom	Ligand Atom	Bond length
ALA 68	H	O	2.23 A
TYR 69	H	O	2.05A
ARG 51	H	O	2.10A
ARG 51	H	O	2.26A
ARG 51	H	O	1.98A

Besides the conformational stability, the potential energy profile was continuously negative in the entire trajectory of simulation indicating stable energetic state and absence of major destabilization structural changes of protein–ligand complex. **(Figure 3a and 3b)**. The RMSD profile recorded reveals that ZINC02123682 was consistently restrained within the MAO-A binding cavity and then sustained a statically predicted mode of docking throughout solvated simulations. Comparison of the conformational states obtained from multiple MB and MD trajectories as well as a Note on using 1 ns long MD simulations for evaluating stability-MD simulation times are significantly smaller than what is generally used for detailed protein–ligand dynamic evaluation thus shedding doubt on its utility in AT modelling. More detailed analyses of binding free-energy and protein flexibility using MM/PBSA or MM/GBSA methods such as RMSF, Rg, SASA, and hydrogen-bond occupancy for ligand stability after long simulations (50–100 ns or more) would give a deeper insight into the conformational dynamics. Thus, although the present MD results offer initial in silico evidence for the stability of the MAO-A–ZINC02123682 complex, longer MD simulations and experimental studies are needed to conclusively demonstrate that this candidate compound is stable and potent as an inhibitor. Together, the pharmacophore, docking, and molecular dynamics findings provide computational support for the potential interaction of ZINC02123682 with MAO-A. These results suggest that the compound may serve as a starting point for further MAO-A inhibitor development; however, its enzymatic potency, selectivity, cellular effects, and neuroprotective potential require experimental validation.

4. Discussion

The present study provides a coherent computational framework for identifying a potential MAO-A inhibitor relevant to diabetic neuropathy, integrating ligand-based pharmacophore modeling, virtual screening, molecular docking, and molecular dynamics (MD) simulation. The rationale for targeting MAO-A is biologically relevant because excessive MAO-A-mediated monoamine oxidation can generate hydrogen peroxide and reactive aldehydes, thereby contributing to oxidative stress, mitochondrial dysfunction, neuroinflammation, and neuronal injury—processes that overlap substantially with the pathological mechanisms described for diabetic neuropathy. Thus, inhibition of MAO-A represents a potentially disease-modifying strategy that could complement existing symptomatic approaches, although the present findings remain computational and require experimental confirmation. The pharmacophore analysis was particularly important for expanding the chemical space beyond the original caffeine-derived compounds. Fifty-two experimentally characterized caffeine derivatives were used to generate 272 hypotheses after extensive conformational sampling. Among these, the five-feature AAHRR model, consisting of two hydrogen-bond acceptors, one hydrophobic feature, and two aromatic-ring features, was selected as the most relevant hypothesis. This arrangement provides a plausible explanation for the molecular requirements governing MAO-A recognition. The hydrogen-bond acceptors may facilitate polar interactions within the binding cavity, whereas the hydrophobic and aromatic components can support complementary nonpolar and aromatic contacts. Importantly, the model enabled the screening of approximately 1,000 compounds from the ZINC database under pharmacophoric and drug-likeness constraints, demonstrating its utility for transferring interaction features identified from caffeine derivatives into a chemically broader virtual library.

An additional strength is the sequential reduction of candidate space: the workflow moved from a literature-derived ligand set to pharmacophore-compatible ZINC molecules and subsequently to 591 compounds with acceptable docking characteristics before selecting the lead. This progressive filtering reduces dependence on a single computational criterion and provides convergent evidence from ligand similarity, three-dimensional feature matching, receptor complementarity, and dynamic stability. Such a strategy is useful for early-stage discovery because it can prioritize experimentally testable molecules while reducing resources required for unfocused biochemical screening. The supplementary

screening data further document the breadth of the searched chemical space. The docking stage further narrowed this chemical space and identified ZINC02123682 as the leading candidate, with a Glide G-score of −7.54. The compound showed compatibility with the AAHRR features and was favorably accommodated within the MAO-A binding cavity. Its predicted interaction network included ALA68, TYR69, and ARG51, with oxygen-mediated hydrogen-bond contacts ranging from 1.98 to 2.26 Å. These short distances are consistent with favorable hydrogen-bond geometry and provide a structural basis for the predicted stabilization of the ligand. The interaction pattern also suggests that the compound may occupy a functionally relevant region of the MAO-A pocket and potentially interfere with substrate recognition. The docking results therefore strengthen the pharmacophore-based prioritization of ZINC02123682 rather than representing an isolated docking hit. The interaction distances and residue-level contacts are also explicitly reported in **Table 2**.

The MD analysis provides an additional dynamic perspective on the docking prediction. During the 1-ns simulation in explicit TIP3P water using the OPLS_2005 force field, the complex displayed RMSD values generally within approximately 2–4 Å, indicating that the system reached and maintained a comparatively stable conformational regime. The consistently negative potential-energy profile further supports the absence of major energetic destabilization during the simulated trajectory. Together, these observations suggest that the docked ligand orientation can be retained under solvated conditions and provide preliminary evidence that the predicted MAO-A–ZINC02123682 complex is dynamically plausible. The trajectory therefore complements the static docking analysis by showing that the predicted interaction is not immediately disrupted during the simulation. Nevertheless, the results should be interpreted as lead-identification evidence rather than proof of inhibitory activity. The AAHRR pharmacophore currently relies mainly on internal model consistency and requires independent validation using experimentally characterized active and inactive compounds, including retrospective metrics such as ROC-AUC, enrichment factor, Güner–Henry score, BEDROC, and external decoy testing. Likewise, the Glide G-score is a relative computational ranking metric and cannot be directly equated with experimental binding affinity or enzyme inhibition. The 1-ns MD simulation is also relatively short for detailed protein–ligand dynamics. Longer simulations of 50–100 ns or more, combined with RMSF, radius of gyration, solvent-accessible surface area, hydrogen-bond occupancy, and MM/GBSA or MM/PBSA analyses, would provide a stronger assessment of stability and binding energetics. Overall, the integrated workflow successfully prioritizes ZINC02123682 as a promising MAO-A lead and provides a mechanistic hypothesis linking its predicted binding to potential reduction of MAO-A-associated oxidative stress. However, its relevance to diabetic neuropathy must be established experimentally through MAO-A inhibition assays, MAO-A/MAO-B selectivity testing, cellular neuroprotection studies, cytotoxicity and ADMET assessment, and ultimately appropriate in vivo validation. The most appropriate interpretation is therefore that ZINC02123682 represents a computationally prioritized starting scaffold for subsequent MAO-A inhibitor optimization, rather than an established therapeutic candidate.

5. Conclusion

The present study demonstrates the potential of an integrated computer-aided drug discovery strategy for identifying novel Monoamine Oxidase A (MAO-A) inhibitor candidates relevant to diabetic neuropathy. By combining ligand-based pharmacophore modeling, pharmacophore-guided virtual screening, molecular docking, and molecular dynamics simulation, the study provides a systematic approach for prioritizing compounds with favorable MAO-A binding characteristics. The analysis of 52 experimentally characterized caffeine derivatives generated 272 pharmacophore hypotheses, from which the five-feature AAHRR model comprising two hydrogen-bond acceptors, one hydrophobic feature, and two aromatic-ring features was identified as the most relevant pharmacophoric arrangement. Application of this pharmacophore model to the ZINC database enabled the identification of approximately 1,000 pharmacophore-compatible compounds, followed by structure-based screening that yielded 591 compounds with acceptable docking characteristics. Among these candidates, ZINC02123682 emerged as the leading compound with a Glide G-score of −7.54. Its predicted binding mode showed favorable interactions with ALA68, TYR69, and ARG51, including hydrogen-bond contacts within the 1.98–2.26 Å range, supporting its favorable accommodation within the MAO-A binding region. Molecular dynamics simulation provided preliminary evidence that the predicted protein–ligand complex remained conformationally stable during the 1-ns simulation. RMSD values remained approximately within 2–4 Å, while the potential-energy profile remained negative throughout the trajectory, suggesting the absence of major structural destabilization under the simulated conditions. These findings strengthen the computational rationale for considering ZINC02123682 as a potential MAO-A lead scaffold. Importantly, the findings should not be interpreted as confirmation of biological activity or therapeutic efficacy. Pharmacophore and docking approaches are subject to limitations associated with receptor flexibility, conformational sampling, and scoring functions, while the relatively short MD simulation provides only preliminary evidence of dynamic stability. Therefore, longer MD simulations, binding free-energy calculations, independent pharmacophore validation, MAO-A inhibition assays, MAO-A/MAO-B selectivity studies, cytotoxicity and ADMET evaluation, and cellular neuroprotection experiments are required. Overall, ZINC02123682 represents a computationally prioritized candidate and a promising starting point for subsequent optimization and experimental development of MAO-A-directed therapeutic strategies for diabetic neuropathy.

6. Disclosure Statements

6.1. Author Contribution

GM: Conceptualization, Methodology, Investigation, Data curation, Formal analysis, Writing–original draft. **SP:** Supervision, Validation, Writing – review & editing, Project administration. **GM** served as the corresponding author and was responsible for overall coordination of the study and manuscript.

6.2. Declaration of Generative AI

The authors used generative artificial intelligence tools solely for language editing and grammatical correction. The AI tools did not contribute to the study design, data collection, analysis, interpretation, or generation of scientific content. All content has been reviewed and approved by the authors, who take full responsibility for the integrity and accuracy of the work.

6.3. Ethics approval (for clinical/animal studies)

This study is entirely computational and does not involve human participants, clinical samples, identifiable personal data, or experimental animals. All analyses were performed using publicly available datasets and in silico methods. Therefore, this study did not require ethical approval in accordance with the guidelines of Bharathiar University and applicable national regulations.

6.4. Informed Consent Statement

This study utilized publicly available datasets that do not contain identifiable personal information. Therefore, informed consent was not required.

6.5. Data Availability Statement

The computational data used and generated from this study are available from the corresponding author upon reasonable request.

6.6. Acknowledgment

None

6.7. Funding Statement

This research received no external funding. All work was conducted using institutional resources without dedicated grant support.

6.8. Conflicts of Interest

The authors declare that they have no known financial, personal, academic, or other relationships that could inappropriately influence, or be perceived to influence, the work reported in this manuscript. All authors confirm that there are no competing interests to declare.

6.9. Corresponding Author Contact Information

The corresponding author **Dr. Gowdham Manivel** can be contacted via email gowdhamgct[at]gmail.com.

6.10. Supplementary Information

Supplementary material is available for this article at https://jomi.aayvu.com/SuppFile/225614/1/

6.11. ORcID Information

Gowdham Manivel	0000-0003-0264-9420
Shanmughavel Piramanayagam	0000-0003-4321-6058

6.12. Handling Editor Information

This manuscript was handled and edited by **Dr. Chandrabose Selvaraj**, Professor, Bioinformatics Division, Department of Marine Biotechnology, AMET University (Academy of Maritime Education and Training) (Deemed to be University), East Coast Road, Kanathur, Chennai, Tamil Nadu – 603112, India. **Editor contact email:** jomi[at]aayvu.com

7. Reference

Adcock SA, McCammon JA. (2006), Molecular dynamics: survey of methods for simulating the activity of proteins, *Chem Rev,* 106(5):1589-615. **doi:**10.1021/cr040426m. **PMID:** 16683746.

Almars AI, Kattan SW. (2025), Identification of novel Menin-MLL interaction inhibitors targeting leukemia using in-silico virtual screening and structure-based drug design approaches, *J Genet Eng Biotechnol,* 23(4):100612. **doi:**10.1016/j.jgeb.2025.100612. **PMID:** 41386877.

Alnajeebi AM. (2026), Molecular docking, DFT analysis, pharmacokinetic profiling and MD simulation of Ilex aquifolium L. flavonoids as potential alpha-glucosidase predicted inhibitors for diabetes, *Sci Rep,* 16(1) **doi:**10.1038/s41598-026-50123-y. **PMID:** 42141107.

Arcon JP, Turjanski AG, Marti MA, Forli S. (2021), Biased Docking for Protein-Ligand Pose Prediction, *Methods Mol Biol,* 2266:39-72. **doi:**10.1007/978-1-0716-1209-5_3. **PMID:** 33759120.

Cagnin S, Brugnaro M, Millino C, Pacchioni B, Troiano C, Di Sante M, Kaludercic N. (2022), Monoamine Oxidase-Dependent Pro-Survival Signaling in Diabetic Hearts Is Mediated by miRNAs, *Cells,* 11(17) **doi:**10.3390/cells11172697. **PMID:** 36078109.

Cediel-Becerra JDD, Silva JCF, Dias R. (2025), EquilibraTor streamlines molecular dynamics simulations in a single execution, *Comput Struct Biotechnol J,* 27:5318-5325. **doi:**10.1016/j.csbj.2025.11.034. **PMID:** 41377122.

Ciancetta A, O'Connor RD, Paoletta S, Jacobson KA. (2017), Demystifying P2Y(1) Receptor Ligand Recognition through Docking and Molecular Dynamics Analyses, *J Chem Inf Model,* 57(12):3104-3123. **doi:**10.1021/acs.jcim.7b00528. **PMID:** 29182323.

Coleman RG, Carchia M, Sterling T, Irwin JJ, Shoichet BK. (2013), Ligand pose and orientational sampling in molecular docking, *PLoS One,* 8(10):e75992. **doi:**10.1371/journal.pone.0075992. **PMID:** 24098414.

Elokely KM, Doerksen RJ. (2013), Docking challenge: protein sampling and molecular docking performance, *J Chem Inf Model,* 53(8):1934-45. **doi:**10.1021/ci400040d. **PMID:** 23530568.

Giordano D, Biancaniello C, Argenio MA, Facchiano A. (2022), Drug Design by Pharmacophore and Virtual Screening Approach, *Pharmaceuticals (Basel),* 15(5) **doi:**10.3390/ph15050646. **PMID:** 35631472.

Gonzalez P, Lozano P, Ros G, Solano F. (2023), Hyperglycemia and Oxidative Stress: An Integral, Updated and Critical Overview of Their Metabolic Interconnections, *Int J Mol Sci,* 24(11) **doi:**10.3390/ijms24119352. **PMID:** 37298303.

Graves SM, Xie Z, Stout KA, Zampese E, Burbulla LF, Shih JC, Kondapalli J, Patriarchi T, Tian L, Brichta L, Greengard P, Krainc D, Schumacker PT, Surmeier DJ. (2020), Dopamine metabolism by a monoamine oxidase mitochondrial shuttle activates the electron transport chain, *Nat Neurosci,* 23(1):15-20. **doi:**10.1038/s41593-019-0556-3. **PMID:** 31844313.

Gupta A, Gupta T, Singh TG, Singh R. (2026), Involvement of cellular and enzymatic aspects in the complexity of diabetic neuropathy, *Tissue Barriers,* 14(2):2581880. **doi:**10.1080/21688370.2025.2581880. **PMID:** 41170890.

Heider J, Kilian J, Garifulina A, Hering S, Langer T, Seidel T. (2023), Apo2ph4: A Versatile Workflow for the Generation of Receptor-based Pharmacophore Models for Virtual Screening, *J Chem Inf Model,* 63(1):101-110. **doi:**10.1021/acs.jcim.2c00814. **PMID:** 36526584.

Hong R, Li X. (2019), Discovery of monoamine oxidase inhibitors by medicinal chemistry approaches, *Medchemcomm,* 10(1):10-25. **doi:**10.1039/c8md00446c. **PMID:** 30774851.

Huang Y, Benni S, Yadav UP, Babu MA, Verma A, Singh TG, Bansal N, Zhang Y. (2026), Deploying the high-throughput virtual screening (HTVS) approach for the identification of new lactate dehydrogenase (LDH) inhibitors with anticancer assets, *Sci Rep,* 16(1):5921. **doi:**10.1038/s41598-026-36385-6. **PMID:** 41565942.

Johnston RC, Yao K, Kaplan Z, Chelliah M, Leswing K, Seekins S, Watts S, Calkins D, Chief Elk J, Jerome SV, Repasky MP, Shelley JC. (2023), Epik: pK(a) and Protonation State Prediction through Machine Learning, *J Chem Theory Comput,* 19(8):2380-2388. **doi:**10.1021/acs.jctc.3c00044. **PMID:** 37023332.

Kaludercic N, Arusei RJ, Di Lisa F. (2023), Recent advances on the role of monoamine oxidases in cardiac pathophysiology, *Basic Res Cardiol,* 118(1):41. **doi:**10.1007/s00395-023-01012-2. **PMID:** 37792081.

Kaludercic N, Carpi A, Nagayama T, Sivakumaran V, Zhu G, Lai EW, Bedja D, De Mario A, Chen K, Gabrielson KL, Lindsey ML, Pacak K, Takimoto E, Shih JC, Kass DA, Di Lisa F, Paolocci N. (2014a), Monoamine oxidase B prompts mitochondrial and cardiac dysfunction in pressure overloaded hearts, *Antioxid Redox Signal,* 20(2):267-80. **doi:**10.1089/ars.2012.4616. **PMID:** 23581564.

Kaludercic N, Mialet-Perez J, Paolocci N, Parini A, Di Lisa F. (2014b), Monoamine oxidases as sources of oxidants in the heart, *J Mol Cell Cardiol,* 73:34-42. **doi:**10.1016/j.yjmcc.2013.12.032. **PMID:** 24412580.

Kasznicki J, Kosmalski M, Sliwinska A, Mrowicka M, Stanczyk M, Majsterek I, Drzewoski J. (2012), Evaluation of oxidative stress markers in pathogenesis of diabetic neuropathy, *Mol Biol Rep,* 39(9):8669-78. **doi:**10.1007/s11033-012-1722-9. **PMID:** 22718504.

Li Y, Peng J, Li P, Du H, Li Y, Liu X, Zhang L, Wang LL, Zuo Z. (2019), Identification of potential AMPK activator by pharmacophore modeling, molecular docking and QSAR study, *Comput Biol Chem,* 79:165-176. **doi:**10.1016/j.compbiolchem.2019.02.007. **PMID:** 30836318.

Mafethe O, Ntseane T, Dongola TH, Shonhai A, Gumede NJ, Mokoena F. (2023), Pharmacophore Model-Based Virtual Screening Workflow for Discovery of Inhibitors Targeting Plasmodium falciparum Hsp90, *ACS Omega,* 8(41):38220-38232. **doi:**10.1021/acsomega.3c04494. **PMID:** 37867657.

Maggiorani D, Manzella N, Edmondson DE, Mattevi A, Parini A, Binda C, Mialet-Perez J. (2017), Monoamine Oxidases, Oxidative Stress, and Altered Mitochondrial Dynamics in Cardiac Ageing, *Oxid Med Cell Longev,* 2017:3017947. **doi:**10.1155/2017/3017947. **PMID:** 28546851.

Manish M, Mishra S, Anand A, Subbarao N. (2022), Computational molecular interaction between SARS-CoV-2 main protease and theaflavin digallate using free energy perturbation and molecular dynamics, *Comput Biol Med,* 150:106125. **doi:**10.1016/j.compbiomed.2022.106125. **PMID:** 36240593.

Mateev E, Georgieva M, Mateeva A, Zlatkov A, Ahmad S, Raza K, Azevedo V, Barh D. (2023), Structure-Based Design of Novel MAO-B Inhibitors: A Review, *Molecules,* 28(12) **doi:**10.3390/molecules28124814. **PMID:** 37375370.

Mukherjee S, Balius TE, Rizzo RC. (2010), Docking validation resources: protein family and ligand flexibility experiments, *J Chem Inf Model,* 50(11):1986-2000. **doi:**10.1021/ci1001982. **PMID:** 21033739.

Olanders G, Alogheli H, Brandt P, Karlen A. (2020), Conformational analysis of macrocycles: comparing general and specialized methods, *J Comput Aided Mol Des,* 34(3):231-252. **doi:**10.1007/s10822-020-00277-2. **PMID:** 31965404.

Pal S, Kumar V, Kundu B, Bhattacharya D, Preethy N, Reddy MP, Talukdar A. (2019), Ligand-based Pharmacophore Modeling, Virtual Screening and Molecular Docking Studies for Discovery of Potential Topoisomerase I Inhibitors, *Comput Struct Biotechnol J,* 17:291-310. **doi:**10.1016/j.csbj.2019.02.006. **PMID:** 30867893.

Picca A, Calvani R, Coelho-Junior HJ, Landi F, Bernabei R, Marzetti E. (2020), Mitochondrial Dysfunction, Oxidative Stress, and Neuroinflammation: Intertwined Roads to Neurodegeneration, *Antioxidants (Basel),* 9(8) **doi:**10.3390/antiox9080647. **PMID:** 32707949.

Poonia P, Sharma M, Jha P, Chopra M. (2023), Pharmacophore-based virtual screening of ZINC database, molecular modeling and designing new derivatives as potential HDAC6 inhibitors, *Mol Divers,* 27(5):2053-2071. **doi:**10.1007/s11030-022-10540-3. **PMID:** 36214962.

Rahimi F, Abbasi M. (2026), 3D-QSAR and free energy landscape analysis for predicting novel JAK3 inhibitors in rheumatoid arthritis therapy, *Sci Rep,* 16(1) **doi:**10.1038/s41598-026-50981-6. **PMID:** 42050339.

Ramachandran R, Piramanyagam S. (2017), Pharmacophore modeling, atom based 3D-QSAR and Molecular docking approaches to screen C-X-C chemokine receptor type 4 antagonists as microbicides for human immunodeficiency virus-1, *Virusdisease,* 28(3):272-280. **doi:**10.1007/s13337-017-0397-1. **PMID:** 29291213.

Ranade SD, Alegaon SG, Khatib NA, Gharge S, Kavalapure RS. (2024), Quinoline-based Schiff bases as possible antidiabetic agents: ligand-based pharmacophore modeling, 3D QSAR, docking, and molecular dynamics simulations study, *RSC Med Chem,* 15(9):3162-79. **doi:**10.1039/d4md00344f. **PMID:** 39149562.

Samsu N. (2021), Diabetic Nephropathy: Challenges in Pathogenesis, Diagnosis, and Treatment, *Biomed Res Int,* 2021:1497449. **doi:**10.1155/2021/1497449. **PMID:** 34307650.

Son SY, Ma J, Kondou Y, Yoshimura M, Yamashita E, Tsukihara T. (2008), Structure of human monoamine oxidase A at 2.2-A resolution: the control of opening the entry for substrates/inhibitors, *Proc Natl Acad Sci U S A,* 105(15):5739-44. **doi:**10.1073/pnas.0710626105. **PMID:** 18391214.

Song NX, Wang YC, Zhao T, Zhang ZS, Liu JC, Chen ZY, Huang YJ, Wang JY, Shen X. (2026), Selective inhibition of monoamine oxidase B represents a therapeutic strategy for diabetic peripheral neuropathy, *Acta Pharmacol Sin,* 47(7):1792-1808. **doi:**10.1038/s41401-026-01764-2. **PMID:** 41857368.

Tavafi M. (2013), Complexity of diabetic nephropathy pathogenesis and design of investigations, *J Renal Inj Prev,* 2(2):59-62. **doi:**10.12861/jrip.2013.20. **PMID:** 25340129.

Teli MK, K RG. (2012), Pharmacophore generation and atom-based 3D-QSAR of N-iso-propyl pyrrole-based derivatives as HMG-CoA reductase inhibitors, *Org Med Chem Lett,* 2(1):25. **doi:**10.1186/2191-2858-2-25. **PMID:** 22747771.

Vilar S, Uriarte E, Santana L, Lorberbaum T, Hripcsak G, Friedman C, Tatonetti NP. (2014), Similarity-based modeling in large-scale prediction of drug-drug interactions, *Nat Protoc,* 9(9):2147-63. **doi:**10.1038/nprot.2014.151. **PMID:** 25122524.

Yang Y, Zhao B, Wang Y, Lan H, Liu X, Hu Y, Cao P. (2025), Diabetic neuropathy: cutting-edge research and future directions, *Signal Transduct Target Ther,* 10(1):132. **doi:**10.1038/s41392-025-02175-1. **PMID:** 40274830.

Yeung AWK, Georgieva MG, Atanasov AG, Tzvetkov NT. (2019), Monoamine Oxidases (MAOs) as Privileged Molecular Targets in Neuroscience: Research Literature Analysis, *Front Mol Neurosci,* 12:143. **doi:**10.3389/fnmol.2019.00143. **PMID:** 31191248.

How to Cite: Manivel, G., & Piramanayagam, S. (2026). Reprogramming MAO-A-driven oxidative stress: Computational discovery of neuroprotective leads for diabetic neuropathy. *Journal of Medico Informatics, 02(03):* 40-48. **doi:** https://doi.org/10.64659/jomi/225614